Supporting Information for

Arixanthomycins A-C: phylogeny-guided discovery of biologically active eDNA-derived pentangular polyphenols

Hahk-Soo Kang and Sean F. Brady*

Laboratory of Genetically Encoded Small Molecules, The Rockefeller University, Howard Hughes Medical Institute, 1230 York Avenue, New York, NY 10065, United States

Table of contents

Materials and methods:

Library screening and phylogenetic analysis of PCR amplicons: The archived and arrayed soil eDNA libraries used in this study were constructed using DNA isolated from desert soils collected in California (AB), Arizona (AZ and AZ25) and Texas (TX). Each library contains $>10^6$ clones, which is predicted to approach saturating the genetic diversity present in each soil microbiome. These libraries are arrayed as 5,000 membered sub-pools to facilitate screening and gene cluster recovery studies.[1] DNA aliquots from the 5,000 membered sub-pools found in each arrayed library were screened using degenerate primers designed to amplify full-length KS_β genes. Each 25 μL PCR reaction contained 50 ng of cosmid DNA, 2.5 μM of each primer (dp:KS_α-TTCGGSGGITTCCAGWSIGCSATG and dp:ACP-TCSAKSAGSGCSAISGASTCGTAICC),[2] 2 mM dNTPs, 1X ThermoPol reaction buffer (New England Biolabs), 0.5 units Taq DNA polymerase and 5% DMSO. PCR was conducted using the following touchdown protocol: denaturation (95 °C, 2 min), 8 touchdown cycles [95 °C, 45 s; 65 °C (−1 °C per cycle), 1 min; 72 °C, 2 min], 35 standard cycles (95 °C, 45 s; 58 °C, 1 min; 72 °C, 2 min) and a final extension step (72 °C, 2 min).[2] The resulting PCR amplicons were gel-purified and sequenced. Approximately 600 bp KS_β gene fragments (corresponding to nucleotides 25-621 of *benB*) from each amplicon were aligned along with the corresponding regions from known KS_β genes using ClustalW. Phylogenetic analysis was performed using MEGA5.1,[3] and 1,000 bootstrap replicates were used to evaluate the robustness of branches in each phylogenetic tree. The Type II polyketide amplicon tree was constructed using minimum evolution tree estimation methods.[4] The eDNA-derived KS_β sequences that were found in the same clade as the KS_β sequences from known pentangular polyphenol biosynthetic gene clusters were used to generate the pentangular polyphenol sub-tree using a maximum likelihood tree estimation method.[5]

Antibacterial assay: Minimal inhibitory concentration (MIC) for arixanthomycin A (**1**), B (**2**) and C (**3**) against *Staphylococcus aureus* USA-300 (MRSA), *Bacillus subtilis* RM125, *Enterococcus faecalis* (VRE) and *E. coli* DRC39 were determined by liquid dilution methods.[6] Each bacterial strain was grown overnight in either brain heart infusion (MRSA and VRE) or LB (*B. subtilis* RM125 and *E. coli* DRC39) liquid media. Each overnight culture was diluted 1,000-fold and transferred to 96-well microtiter plates (75 μl/well). Compounds were dissolved in DMSO, added into the respective media at 50 μg/ml and serially diluted 2-fold across the plate (50 – 0.02 μg/ml concentrations). These solutions (75 μl) were then transferred to the appropriate well in an assay plate and incubated at 30 °C overnight. Bacterial growth was visually inspected and the last well with no bacterial growth was defined as a MIC.

Antiproliferative assay: The cytotoxicity of arixanthomycins A (**1**), B (**2**) and C (**3**) was evaluated using the colon carcinoma cell line HCT-116 (ATCC; CCL-247),[7] the colorectal adenocarcinoma cell line WiDr (ATCC; CCL-218)[8] and the breast adenocarcinoma cell line MDR-MB-231 (ATCC; HTB-26).[9] HCT-116 cells were grown in McCoy's 5A Modified Medium (Gibco) supplemented with 10% (v/v) FBS. WiDr and MDA-MB-231 cells were grown in DMEM Medium (Gibco) supplemented with 10% (v/v) FBS. Cells in log phase growth were harvested by trypsinization. Trypsinized cells were seeded onto 96-well plates (HCT-116: 1,000 cells/well, WiDr: 3,000 cells/well, MDA-MB-231: 8,000 cells/well) and incubated overnight at 37 °C in the presence of 5% CO_2. Compounds **1** – **3** (in DMSO) were sequentially diluted (2 or 3-fold dilutions starting at 50 μg/ml) across a 96-well plate and 100 μL was transferred to the appropriate well in an assay plate. Doxorubicin (Sigma-Aldrich) was used as a positive control and DMSO was used as a negative control. The plates were incubated at 37 °C for 3 days and then evaluated for viability using crystal violet- and MTT-based colorimetric assays.[10-11] Cell viability was recorded based on the percent stain present in each well relative to no drug DMSO control wells.

Supplementary Discussion 1. Structure determination of arixanthomycins A – C (**1** – **3**)

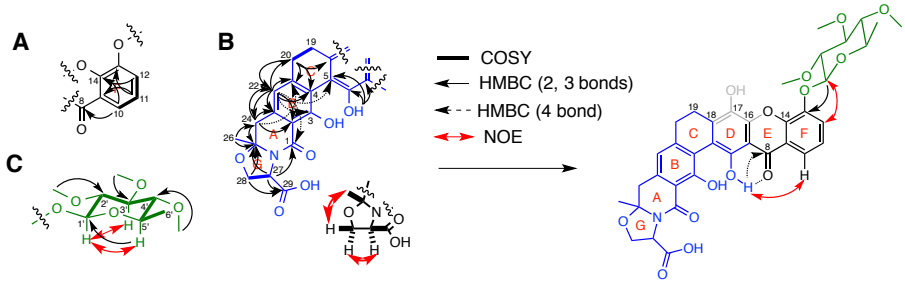

Supplementary figure 1. 2D NMR correlations used to determine the structure of arixanthomycin A (**1**).

Overview: The structures of arixanthomycins A (**1**), B (**2**) and C (**3**) were determined by a combined analysis of HRESIMS, and 1D and 2D NMR data. The HRESIMS spectrum of **1** displayed a pseudo molecular ion peak at 720.2300 $[M+H]^+$, suggesting the molecular formula of **1** as $C_{37}H_{37}NO_{14}$. The odd molecular weight indicated the presence of a nitrogen atom in **1**. Line broadening was observed for several ^1H and ^{13}C NMR signals at room temperature. These broad signals were significantly sharpened at elevated temperatures (100°C), indicating the possibility of a conformational interchange at room temperature. Due to line broadening at room temperature, NMR data were acquired at 100°C. The ^1H NMR spectrum showed a signal distribution characteristic of a glycosylated aromatic compound, including phenolic hydroxyls (10 – 15 ppm), aromatic protons (6 – 8 ppm), a sugar anomeric proton (5 – 6 ppm) and oxygenated methine protons (3 – 5 ppm). Analysis of the 2D NMR spectra including COSY, HMQC and HMBC established three sub-structures designated as A, B and C (supplementary figure 1).

Substructure A: COSY correlations between H-10(δ_H 7.89)/H-11(δ_H 7.42)/H-12(δ_H 7.63), as well as HMBC correlations from H-10 and H-12 to C-14 (δ_C 145.8), from H-11 to C-9 (δ_C 121.2) and C-13 (δ_C 145.2), and from H-10 to C-8 (δ_C 181.1) indicated the presence of an aromatic ring (ring F) substituted with hydroxyls at C-13 and C-14 and a ketone at C-9.

Substructure B: A COSY correlation between H_2-28 (δ_H 4.18 and 4.54) and H-27 (δ_H 4.76), together with HMBC correlations from H-28 to C-25 (δ_C 93.3) and C-29 (δ_C 170.1), H-27 to C-1 (δ_C 164.4), C-25 and C-29 and from H-26 to C-24 and C-25 determined the structure of an oxazolidine ring (ring G) functionalized with a carboxyl group at C-27 and a methyl and methylene at C-25. This oxazolidine ring was expanded to include a lactam (ring A) and aromatic rings (ring B) by HMBC correlations from H-22 (δ_H 6.81) to C-2 (δ_C 108.4), C-4 (δ_C 118.4), C-20 (δ_C 29.2), C-21 (δ_C 146.1), C-23 (δ_C 134.7) and C-24 (δ_C 39.3), from H_2-20 (δ_H 2.62 and 2.75) to C-4 and C-21, and from H_2-24 (δ_H 3.18) to C-2 and C-23. A COSY correlation between H_2-19 (δ_H 2.63 and 3.10) and H_2-20 (δ_H 2.62 and 2.75), in combination with an HMBC correlation from H_2-20 to C-18 (δ_C 138.4), further expanded this partial structure with two aliphatic (C-19 and C-20) and one olefinic (C-18) carbons. HMBC correlations from 6-OH (δ_H 12.70) to C-5 (δ_C 113.2), C-6 (δ_C 150.5) and C-7 (δ_C 106.7), and a weak four bond HMBC correlations from H-22 to C-5 and C-3 (δ_C 157.6) closed the ring C, establishing substructure B. The relative configuration of the oxazolidine (G ring) was deduced by NOE correlations. An NOE correlation observed between H_3-26 (δ_H 1.47) and H-28a (δ_H 4.18), and between H-28b and H-27 indicated "syn" relationship between methyl (C-26) and carboxylate (C-29).

Substructure C: Substructure C was determined to be a sugar moiety through COSY and HMBC correlations. COSY correlation relay of H-1'(δ_H 5.28)/H-2'(δ_H 3.41)/H-3'(δ_H 3.32)/H-4'(δ_H 2.94)/H-5'(δ_H 3.63)/H-6'(δ_H 1.27), together with an HMBC correlation from H-5' to C-1' (δ_C 100.3), confirmed that the sugar moiety was a deoxysugar. The three methoxy

signals (δ_H 3.52, 3.59 and 3.75) identified in the ^{1}H NMR spectrum showed HMBC correlations to H-2', H-3' and H-4', indicating that all of the hydroxyl groups in the sugar moiety were methylated. The large coupling constants observed between H-1' and H-2' (7.6 Hz), H-2' and H-3' (8.8 Hz), H-3' and H-4' (9.1 Hz), and H-4' and H-5' (9.1 Hz) placed all the methoxy groups in an equatorial position, which were further supported by NOE correlations between H-1' and H-3', and between H-1' and H-5', making substructure C a tri-methylated quinovose.

Connecting the substructures: Substructures A through C were connected via HMBC (Supplementary Figure 1, right, black arrows) and NOE (Supplementary Figure 1, right, red arrows) correlations. An HMBC correlation from H-1' to C-13 connected sub-structures A and C through an *O*-glycosidic bridge. A weak four bond HMBC correlations observed from 6-OH to C-8 and an NOE correlation between 6-OH and H-10 provided a connection between C-7 and C-8. The sharp signal observed for 6-OH is predicted to be the result of hydrogen bonding between the hydrogen of the 6-OH and the oxygen of the C-8 ketone. No further HMBC correlations were observed leaving two carbons (C-16 and C-17) unassigned. The carbon chemical shifts of C-16 (δ_C 144.5) and C-17 (δ_C 132.1) suggested that these carbons were likely to be hydroxylated olefins. The degree of unsaturation calculated from the predicted molecular formula ($C_{37}H_{37}NO_{14}$) was 20, which is two more than that calculated from the partial structure without C-16 and C-17, indicating the presence of one additional ring and one additional double bond. These two isolated carbons were therefore placed between 14-O and C-18, and a hydroxy group was attached to C-17, forming an additional aromatic ring with all the carbons functionalized. This final heptacyclic glycosylated structure satisfies the degree of unsaturation as well as all the spectroscopic data we collected, including HRESIMS, ^{1}H, ^{13}C and 2D NMR data.

Arixanthomycins B and C: The structures of compounds **2** and **3** were determined in the same way as described for **1**. The ^{1}H, ^{13}C and 2D NMR data for **2** and **3** were similar to those for **1**, however both lacked signals for the sugar moiety. HRESIMS predicted molecular formulas for **2** as $C_{29}H_{24}NO_{10}$ (546.1379 $[M+H]^+$) and **3** as $C_{28}H_{22}NO_{10}$ (532.1246 $[M+H]^+$), confirming the absence of the sugar moiety in each molecule. As suggested by the difference in molecular formulas predicted for **2** and **3** ($-CH_2$), the ^{1}H and ^{13}C NMR spectra of **2** displayed an additional methoxy signal (δ_H 3.95; δ_C 61.0) compared to **3**. An HMBC correlation from the methoxy protons to C-17 (δ_C 135.5) placed the methoxy group at C-17 on compound **2**. All other analytic data we collected for compounds **2** and **3** suggested that they were otherwise identical to each other. The structure of **3** was therefore determined to be the aglycone of **1**, and the structure of **2** was determined to be the C-17 methoxylated aglycone of **1**.

Atropisomers: The line broadening seen for some ^{1}H and ^{13}C signals in the NMR spectra collected at room temperature is likely due to two atropisomers slowly interconverting, as has been proposed for the structurally related compound FD-594 (supplementary figure 2).[14]

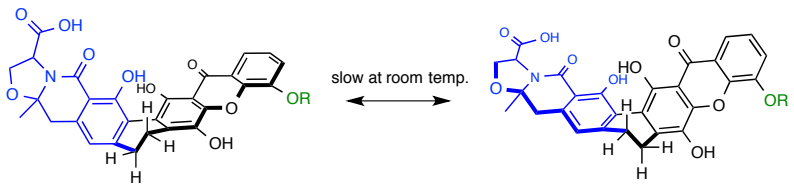

Supplementary figure 2. Atropisomerism of the arixanthomycins likely responsible for line broadening seen in NMR spectra recorded at room temperature.

Supplementary table 1: NMR spectroscopic data (500 MHz at 100°C) for arixanthomycin A (**1**) in DMSO-d_6

No.	Arixanthomycin A (**1**)				
	δ_C [b]	δ_H [a]	*J* in Hz	HMBC	NOE
1	164.4				
2	108.4				
3	157.6				
4	118.4				
5	113.2				
6	150.5				
7	106.7				
8	181.1				
9	121.2				
10	117.8	7.89	dd (7.8, 1.4)	8, 9, 14	
11	123.5	7.42	t (7.8)	10, 12, 13	
12	120.8	7.63	dd (7.8, 1.4)	10, 13, 14	
13	145.2				
14	145.8				
16	144.5				
17	132.1				
18	138.4				
19	23.3	2.63 3.10	m m		
20	29.2	2.62 2.75	m m	4, 18, 21,22	
21	146.1				
22	117.0	6.81	s	1, 2, 3, 4, 20, 21, 23, 24	H-24
23	134.7				
24	39.3	3.18	s	2, 21,22, 23, 25, 26	
25	93.3				
26	22.2	1.47	s	24, 25	
27	56.0	4.76	dd (7.8, 6.2)	1, 13, 25, 28, 29	H-28
28	66.9	4.18 4.54	dd (8.8, 6.2) t (8.8, 7.8)	25, 27, 29	H-27 H-26, H-27
29	170.1				
6-OH		12.7	brs		H-10
1’	100.3	5.28	d (7.6)	13, 2’, 5’	H-12, H-3’, H-5’
2’	84.7	3.41	dd (8.8, 7.6)	2’-OMe, 1’, 3’ 4’	
3’	83.0	3.32	dd (9.1, 8.8)	3’-OMe, 2’, 4’	
4’	84.0	2.94	t (9.1)	4’-OMe, 2’, 5’	
5’	70.1	3.63	dd (9.1, 6.2)	1’	
6’	17.1	1.27	d (6.2)	4’, 5’	
2’-OMe	59.7	3.75	s	2’	
3’-OMe	59.1	3.59	s	3’	
4’-OMe	59.0	3.52	s	4’	

[a]recorded at 500 MHz, [b]recorded at 125 MHz, [a,b]recorded at 373K and signals were referenced to the DMSO-d_6 solvent signals (δ_H 2.50 and δ_H 39.51)

Supplementary table 2: NMR spectroscopic data (600 MHz at room temperature) for arixanthomycins B (**2**) and C (**3**) in DMSO-d_6

No.	arixanthomycin B (**2**)			arixanthomycin C (**3**)		
	δ_C[b]	δ_H[a]	*J* in Hz	δ_C[b]	δ_H[a]	*J* in Hz
1	164.5			nd		
2	108.5[c]			108.5		
3	157.7[c]			nd		
4	118.2[c]			118.2		
5	113.3			113.3		
6	153.3			149.8		
7	107.1			106.5		
8	181.8			181.9		
9	120.9[d]			120.9		
10	114.5	7.64	dd (7.9, 1.3)	114.9	7.64	dd (7.7, 1.3)
11	124.3	7.32	t (7.9)	124.4	7.34	t (7.6)
12	120.8[d]	7.41	dd (7.9, 1.3)	120.7	7.38	dd (7.7, 1.3)
13	146.5			146.1		
14	144.9			144.3		
16	147.5			nd		
17	135.5			nd		
18	142.6			135.4		
19	23.3	nd		nd	nd	
20	29.3	2.59[c] 2.83[c]	brm brm	29.3	2.59[c] 2.83[c]	brm brm
21	146.4			nd		
22	117.5[c]	6.84	brs	117.5	6.83	brs
23	135.2			135.1		
24	39.5	3.20 3.22	d (14.9) d (14.9)	39.4	3.20 3.22	d (13.1) d (13.1)
25	93.5[c]			93.3		
26	22.4	1.42	s	22.4	1.42	s
27	56.2	4.72	dd (8.6, 6.8)	56.4	4.72	dd (8.5, 6.9)
28	67.1	4.14 4.56	dd (8.6, 6.8) t (8.6)	67.2	4.14 4.56	dd (8.5, 6.9) t (8.5)
29	170.6			170.8		
6-OH		13.18	s		12.70	s
13-OH		10.66	s		10.12	s
17-OH					9.28	s
17-OMe	61.0	3.95	s			

[a]recorded at 600 MHz, [b]recorded at 150 MHz, [a,b]signals were referenced to the DMSO-d_6 solvent signals (δ_H 2.50 and δ_H 39.51), [c]broad signals,, [d]interchangeable, [nd]not assigned due to the line broadening of signals

Supplementary Discussion 2. The proposed biosynthesis of arixanthomycins A – C (**1** – **3**)

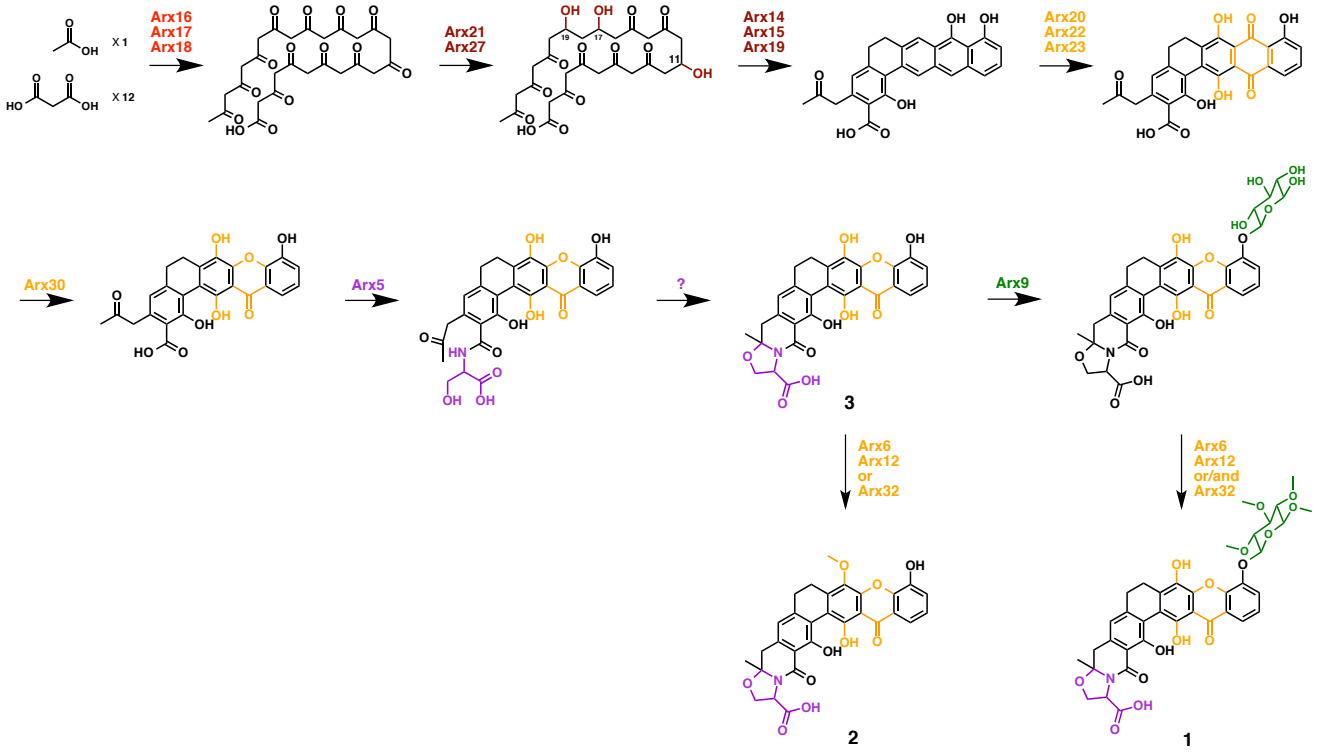

Supplementary figure 3. Our proposed biosynthetic pathway for arixanthomycins A – C (**1** – **3**). This biosynthetic scheme was inferred from general enzyme function predictions and Pfam domain analysis of genes found in the ARX cluster. The order of the proposed steps is not clear.

Supplementary table 3: Gene annotation table for the eDNA-derived ARX (arixanthomycin) gene cluster

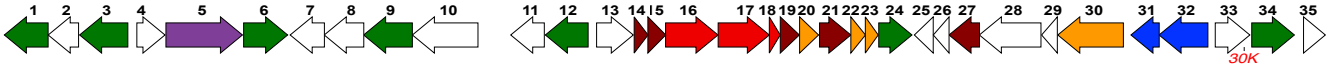

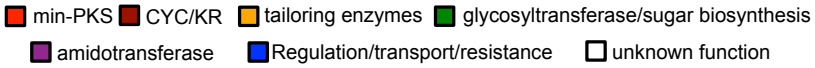

Gene	Size (bp)	Proposed function	Homologous gene	Origin	Identity/ Similarity (%)	Accession NO.
Arx1	1,059	NAD-dependent epimerase/dehydratase		*Streptomyces flavogriseus* ATCC 33331	61/70	YP_004926854.1
Arx2	735	Hypothetical protein		*Streptomyces sp.* MspMP-M5	64/77	WP_018542701.1
Arx3	1,167	Glycosyltransferase	xanG	*Streptomyces flavogirseus*	50/60	ADE22284.1
Arx4	681	Short-chain dehydrogenase/reductase SDR	xanS2	*Streptomyces flavogriseus*	58/69	ADE22303.1
Arx5	1,851	Amidotransferase	pdmN	*Actinomadura hibisca*	48/62	ABK58686.1
Arx6	1,065	O-methyltransferase	sanN	*Streptomyces sp. SANK 61196*	49/61	ADG86324.1
Arx7	828	ABC transporter		*Streptomyces himastatinicus*	49/66	WP_009715426.1
Arx8	957	ABC transporter ATP-binding protein		*Streptomyces coelicoflavus*	60/75	WP_007444312.1
Arx9	1,063	Glycosyltransferase		*Streptomyces sp.* MspMP-M5	47/61	WP_018542716.1
Arx10	1,587	FAD-binding monooxygenase	xanO5	*Streptomyces flavogriseus*	44/59	ADE22302.1
Arx11	813	Hypothetical protein		*Nocardiopsis potens*	32/44	WP_017596478.1
Arx12	1,035	O-methyltransferase		*Actinosynnema mirum DSM 43827*	44/59	YP_003100841.1
Arx13	888	Dehydrogenase	xanS1	*Streptomyces flavogriseus*	58/68	ADE22281.1
Arx14	336	Cyclase	llpCIII	*Streptomyces tendae*	81/92	CAM34347.1
Arx15	432	Cyclase	lpCII	*Streptomyces tendae*	75/83	CAM34346.1
Arx16	1,269	Beta-ketoacyl synthase alpha	llpF	*Streptomyces tendae*	81/88	CAM34345.1
Arx17	1,239	Beta-ketoacyl synthase beta	rubB	*Streptomyces colinus*	73/81	AAG03068.1
Arx18	264	Acyl carrier protein		Uncultured bacterium esnapd17	52/73	AGS49863.1
Arx19	462	Cyclase	rubF	*Streptomyces collinus*	65/77	AAG03070.2
Arx20	459	Monooxygenase	llpB	*Streptomyces tendae*	63/72	CAM34341.1
Arx21	759	3-oxoacyl-ACP reductase	llpZI	*Streptomyces tendae*	73/82	CAM34340.1
Arx22	354	Monooxygenase	llpOIII	*Streptomyces tendae*	70/83	CAM34339.1
Arx23	312	Monooxygenase	xanO6	*Streptomyces flavogriseus*	56/68	ADE22309.1
Arx24	804	NDP-4-ketoreductase	cmmUII	*Streptomyces griseus subsp.*	55/69	CAE17523.1
Arx25	456	Hypothetical protein	llpQ	*Streptomyces tendae*	62/72	CAM34365.1
Arx26	381	Hypothetical protein	llpV	*Streptomyces tendae*	80/88	CAM34369.1
Arx27	738	3-oxoacyl-ACP reductase	llpZIII	*Streptomyces tendae*	68/78	CAM34370.1
Arx28	1,491	Putative peptide transporter	xanQ	*Streptomyces flavogriseus*	53/70	ADE22293.1
Arx29	381	CurD-like protein	xanT	*Streptomyces flavogriseus*	67/79	ADE22317.1
Arx30	1,587	FAD-binding monooxygenase	xanO4	*Streptomyces flavogriseus*	61/75	ADE22300.1
Arx31	684	LuxR family transcriptional regulator		*Nonomuraea coxensis*	70/80	WP_020545909.1
Arx32	1,182	Two-component system histidine kinase		*Nonomuraea coxensis*	44/59	WP_020542953.1
Arx33	837	F420-dependent reductase	xanZ1	*Streptomyces flavogriseus*	49/64	ADE22295.1
Arx34	1,032	Putative methyltransferase	xanM3	*Streptomyces flavogriseus*	47/64	ADE22301.1
Arx35	528	Biotin carboxyl carrier protein	xanB2	*Streptomyces flavogriseus*	45/58	ADE22307.1

References for supplementary material:

1. Brady, S. F. (2007) Construction of soil environmental DNA cosmid libraries and screening for clones that produce biologically active small molecules, *Nat. Protoc.* 2, 1297-305.
2. Seow, K. T.; Meurer, G.; Gerlitz, M.; Wendt-Pienkowski, E.; Hutchinson, C. R.; Davies, J. (1997) A study of iterative type II polyketide synthases, using bacterial genes cloned from soil DNA: a means to access and use genes from uncultured microorganisms, *J. Bacteriol.* 179, 7360-8.
3. Tamura, K.; Peterson, D.; Peterson, N.; Stecher, G.; Nei, M.; Kumar, S. (2011) MEGA5: molecular evolutionary genetics analysis using maximum likelihood, evolutionary distance, and maximum parsimony methods, *Mol. Biol. Evol.* 28, 2731-9.
4. Rzhetsky, A.; Nei, M. (1993) Theoretical foundation of the minimum-evolution method of phylogenetic inference, *Mol. Biol. Evol.* 10, 1073-95.
5. Felsenstein, J. (1981) Evolutionary trees from DNA sequences: a maximum likelihood approach, *J. Mol. Evol.* 17, 368-76.
6. Li, C.; Zhang, F.; Kelly, W. L. (2011) Heterologous production of thiostrepton A and biosynthetic engineering of thiostrepton analogs, *Mol. Biosyst.* 7, 82-90.
7. Brattain, M. G.; Fine, W. D.; Khaled, F. M.; Thompson, J.; Brattain, D. E. (1981) Heterogeneity of malignant cells from a human colonic carcinoma, *Cancer Res.* 41, 1751-6.
8. Noguchi, P.; Wallace, R.; Johnson, J.; Earley, E. M.; O'Brien, S.; Ferrone, S.; Pellegrino, M. A.; Milstien, J.; Needy, C.; Browne, W.; Petricciani, J. (1979) Characterization of the WIDR: a human colon carcinoma cell line, *In Vitro* 15, 401-8.
9. Brinkley, B. R.; Beall, P. T.; Wible, L. J.; Mace, M. L.; Turner, D. S.; Cailleau, R. M. (1980) Variations in cell form and cytoskeleton in human breast carcinoma cells in vitro, *Cancer Res.* 40, 3118-29.
10. Supino, R. (1995) MTT assays, *Methods Mol. Biol.* 43, 137-49.
11. Zivadinovic, D.; Gametchu, B.; Watson, C. S. (2005) Membrane estrogen receptor-alpha levels in MCF-7 breast cancer cells predict cAMP and proliferation responses, *Breast Cancer Res.* 7, R101-12.
12. Asai, Y.; Nonaka, N.; Suzuki, S.; Nishio, M.; Takahashi, K.; Shima, H.; Ohmori, K.; Ohnuki, T.; Komatsubara, S. (1999) TMC-66, a new endothelin converting enzyme inhibitor produced by Streptomyces sp. A5008, *J. Antibiot.* 52, 607-12.
13. Hosokawa, S.; Fumiyama, H.; Fukuda, H.; Fukuda, T.; Seki, M.; Tatsuta, K. (2007) The first total synthesis and structural determination of TMC-66, *Tetrahedron Lett.* 48, 7305-08.
14. Eguchi, T.; Kondo, K.; Kakinuma, K.; Uekusa, H.; Ohashi, Y.; Mizoue, K.; Qiao, Y. F. (1999) Unique Solvent-Dependent Atropisomerism of a Novel Cytotoxic Naphthoxanthene Antibiotic FD-594, *J. Org. Chem.* 64, 5371-76.

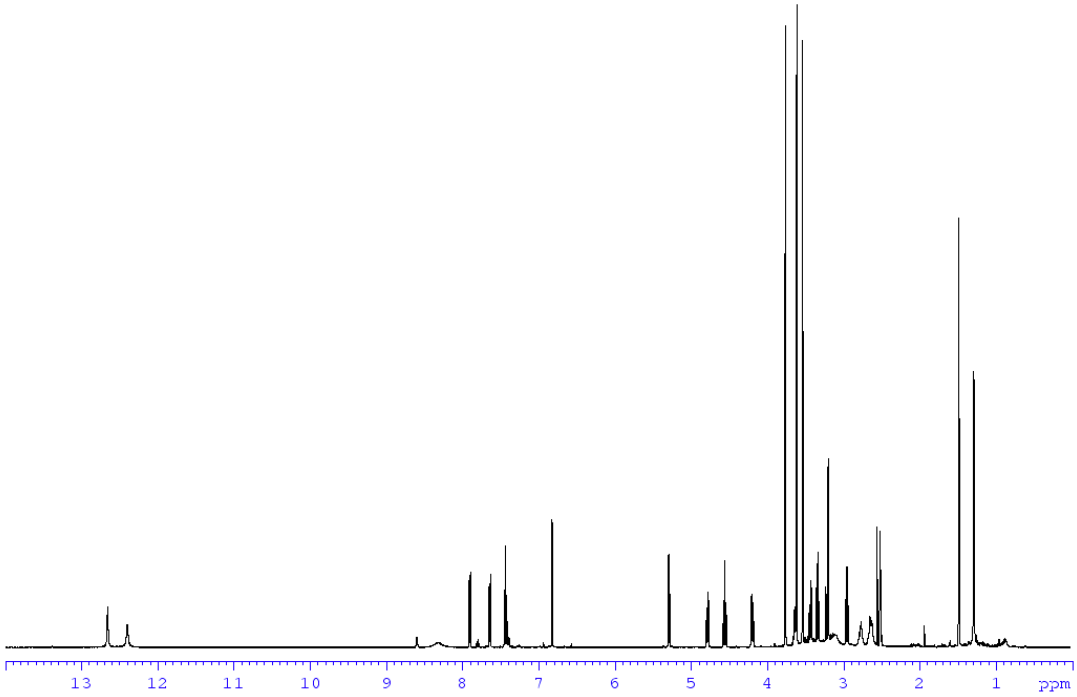

Supplementary figure 4. ^{1}H NMR spectrum (DMSO-d_6, 500 MHz at 100°C) of arixanthomycin A (**1**).

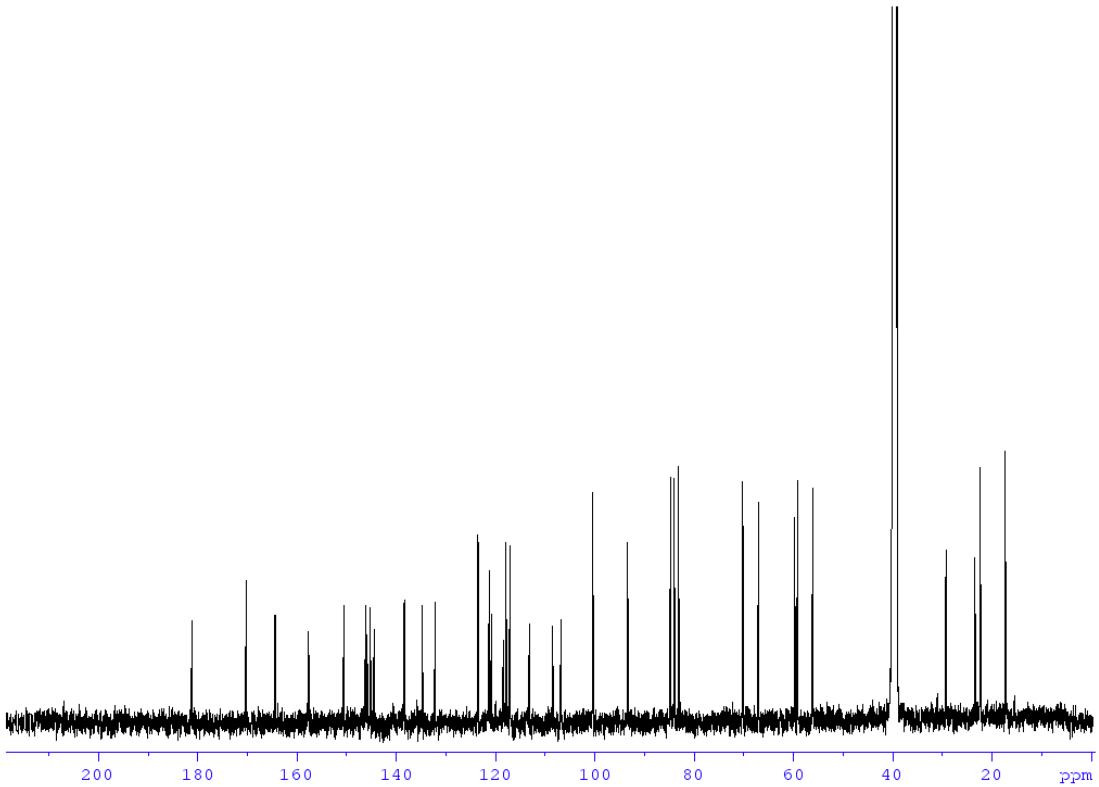

Supplementary figure 5. ^{13}C NMR spectrum (DMSO-d_6, 125 MHz at 100°C) of arixanthomycin A (**1**).

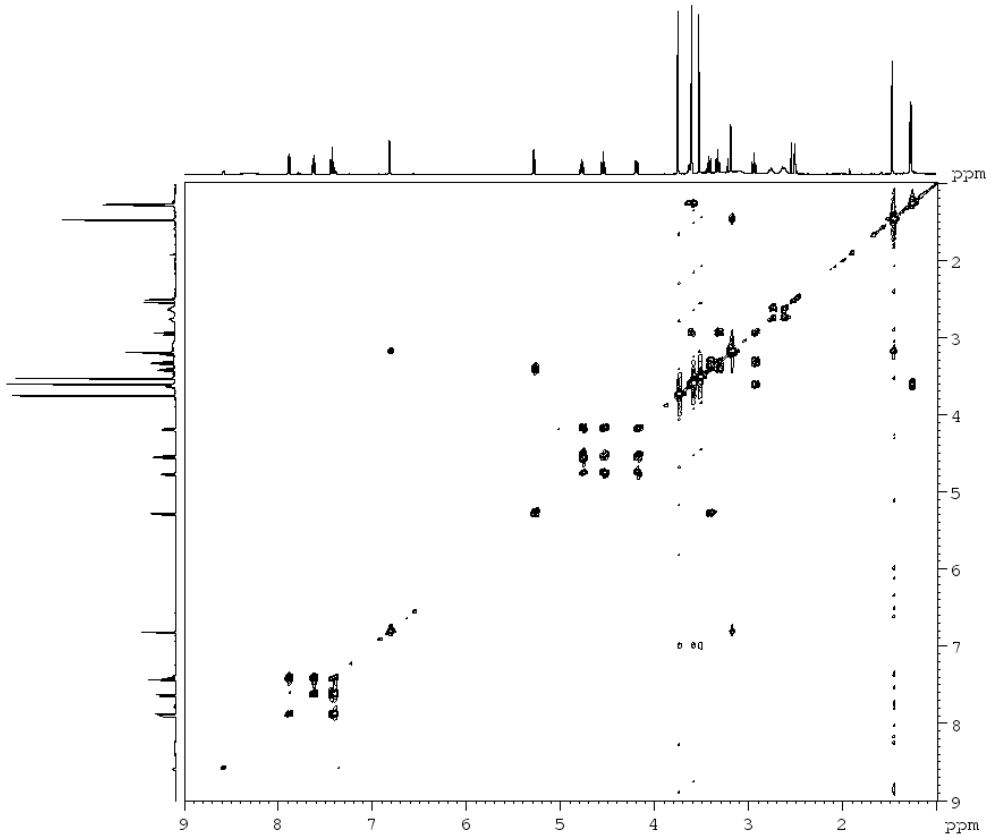

Supplementary figure 6. COSY spectrum (DMSO-d_6, 500 MHz at 100°C) of arixanthomycin A (**1**).

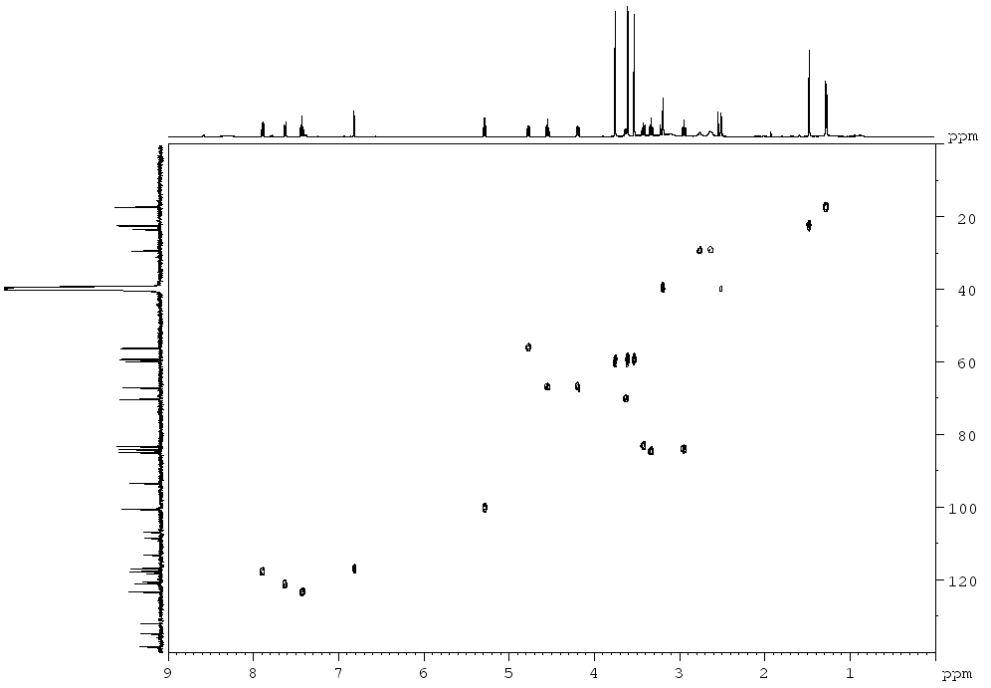

Supplementary figure 7. HMQC spectrum (DMSO-d_6, 500 MHz at 100°C) of arixanthomycin A (**1**).

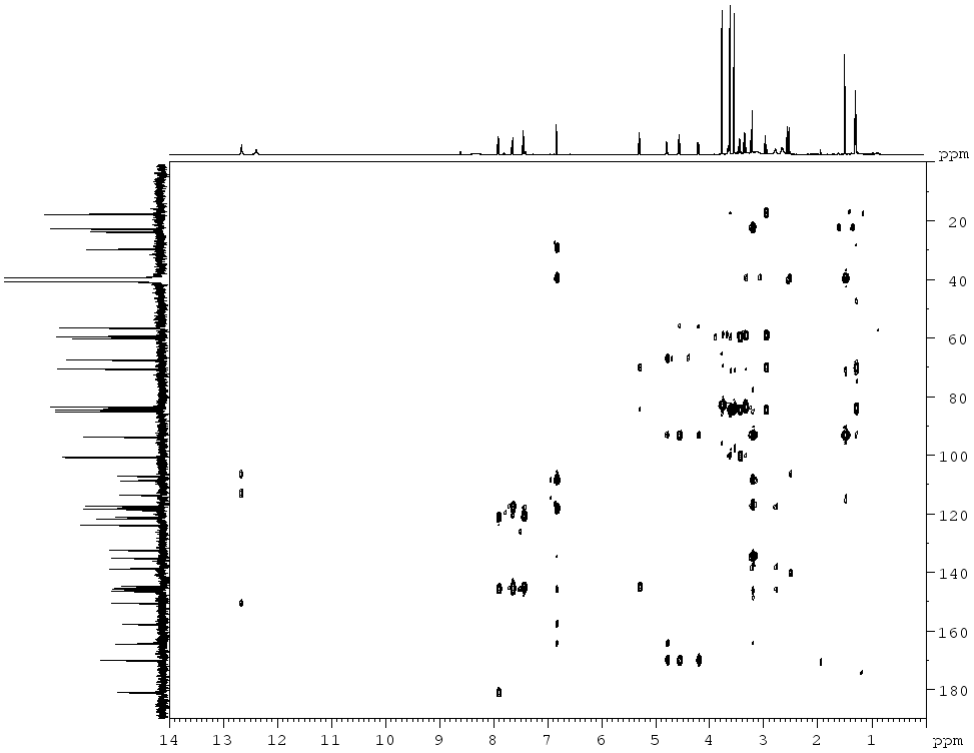

Supplementary figure 8. HMBC spectrum (DMSO-d_6, 500 MHz at 100°C) of arixanthomycin A (**1**).

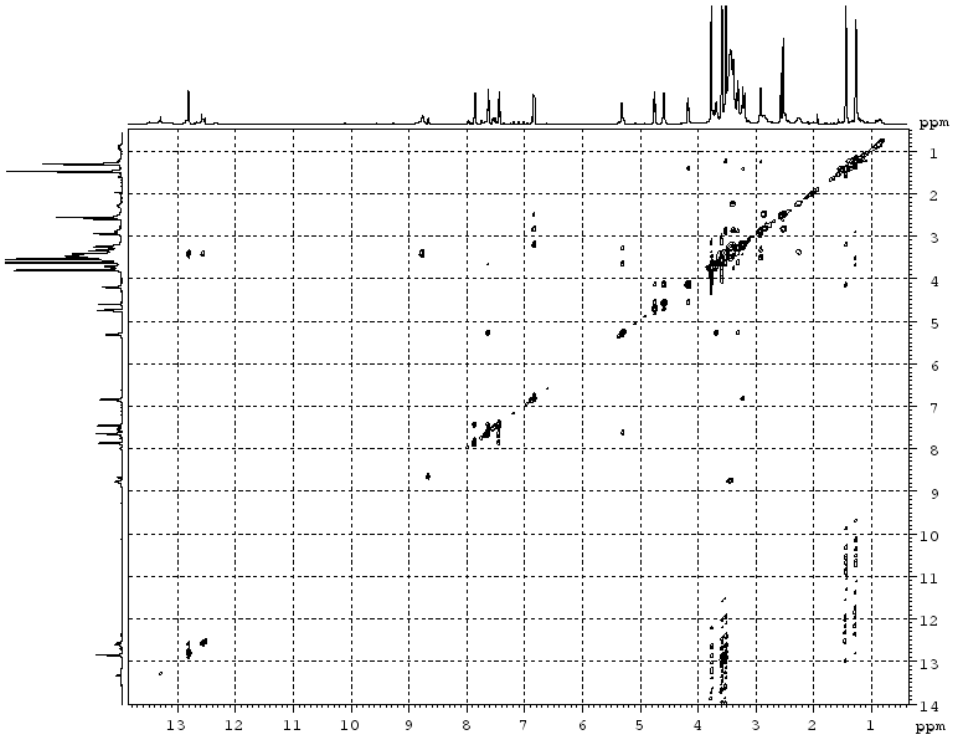

Supplementary figure 9. NOESY spectrum (DMSO-d_6, 600 MHz, mixing time: 600 ms) of arixanthomycin A (**1**).

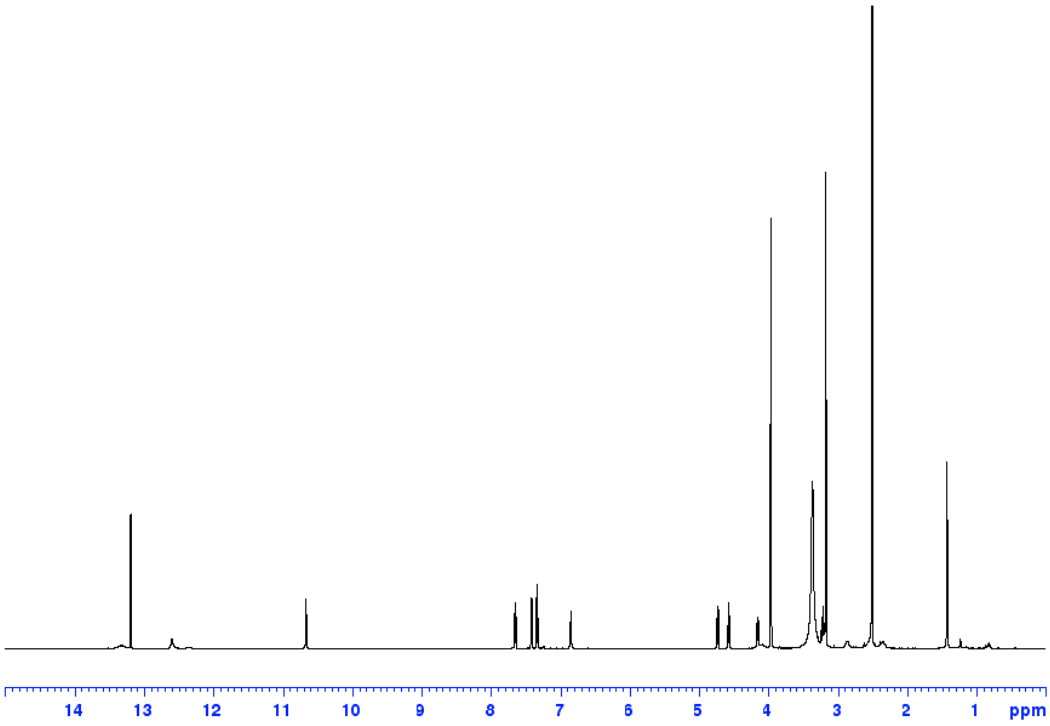

Supplementary figure 10. ^{1}H NMR spectrum (DMSO-d_6, 600 MHz) of arixanthomycin B (**2**).

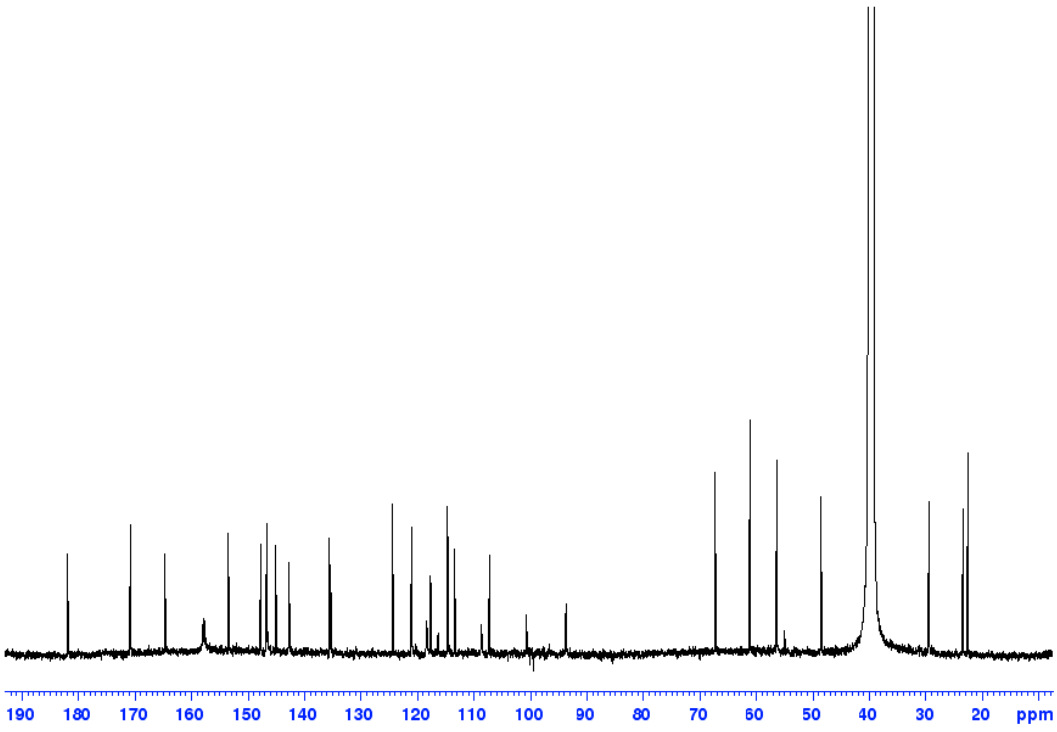

Supplementary figure 11. ^{13}C NMR spectrum (DMSO-d_6, 150 MHz) of arixanthomycin B (**2**).

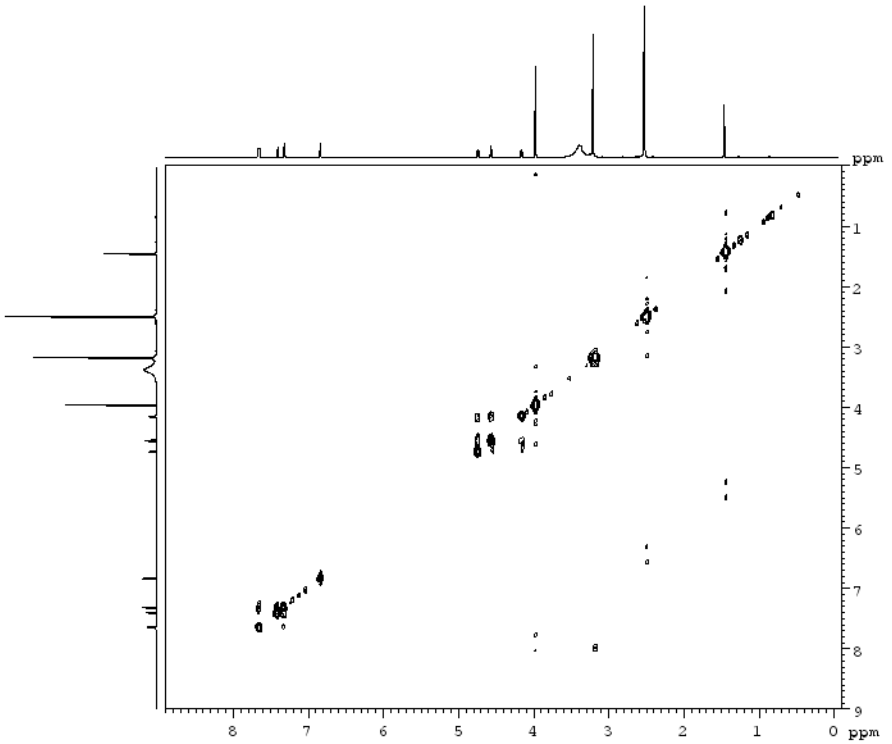

Supplementary figure 12. COSY spectrum (DMSO-d_6, 600 MHz) of arixanthomycin B (**2**).

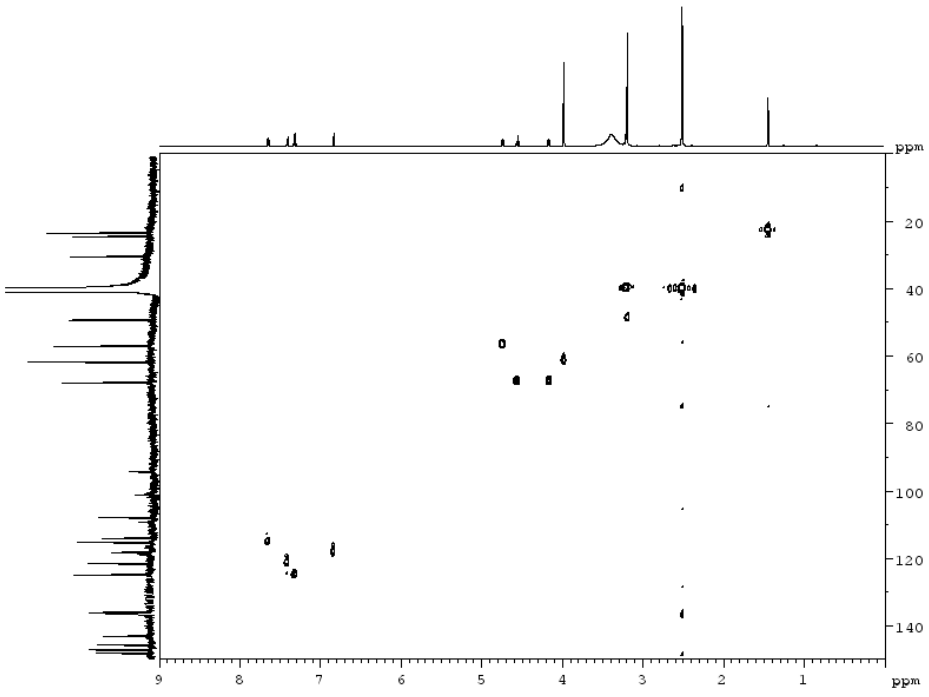

Supplementary figure 13. HMQC spectrum (DMSO-d_6, 600 MHz) of arixanthomycin B (**2**).

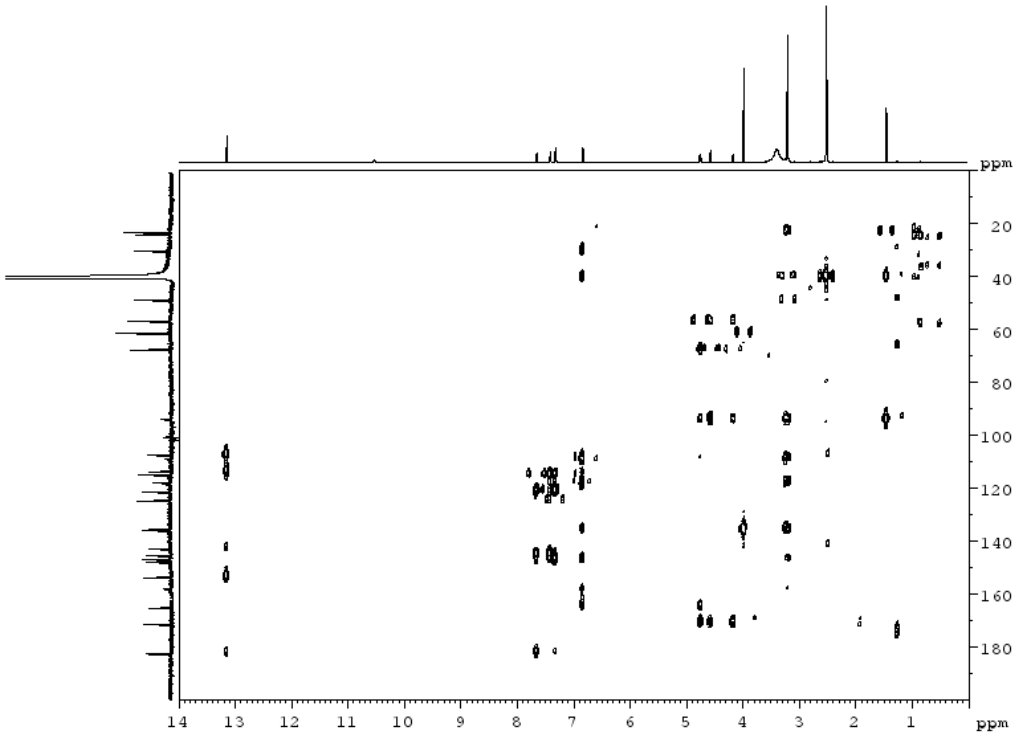

Supplementary figure 14. HMBC spectrum (DMSO-d_6, 600 MHz) of arixanthomycin B (**2**).

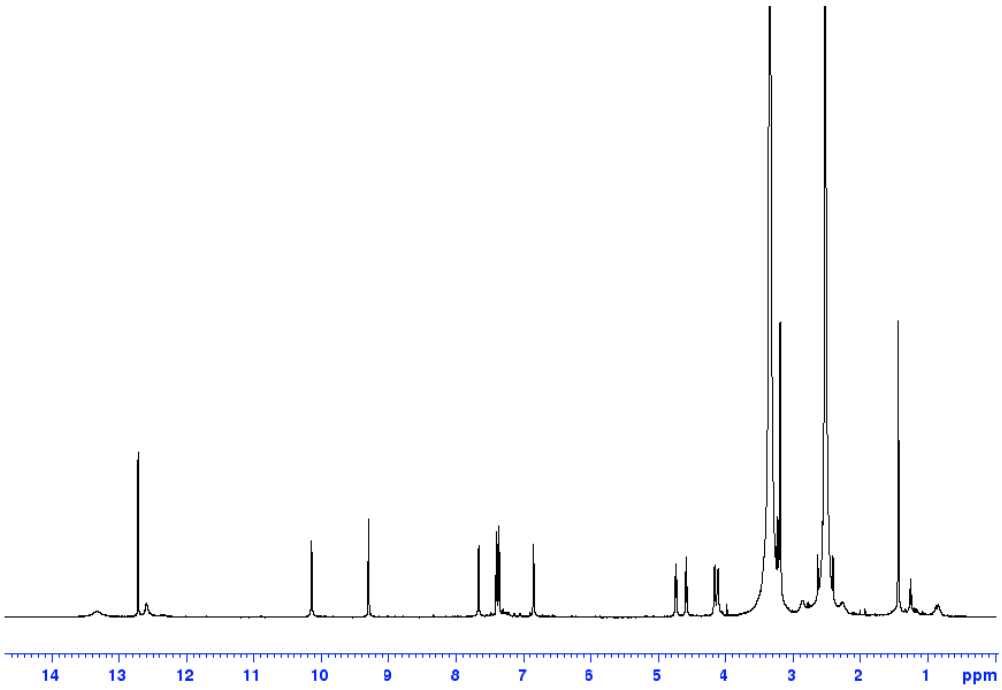

Supplementary figure 15. ^{1}H NMR spectrum (DMSO-d_6, 600 MHz) of arixanthomycin C (**3**).

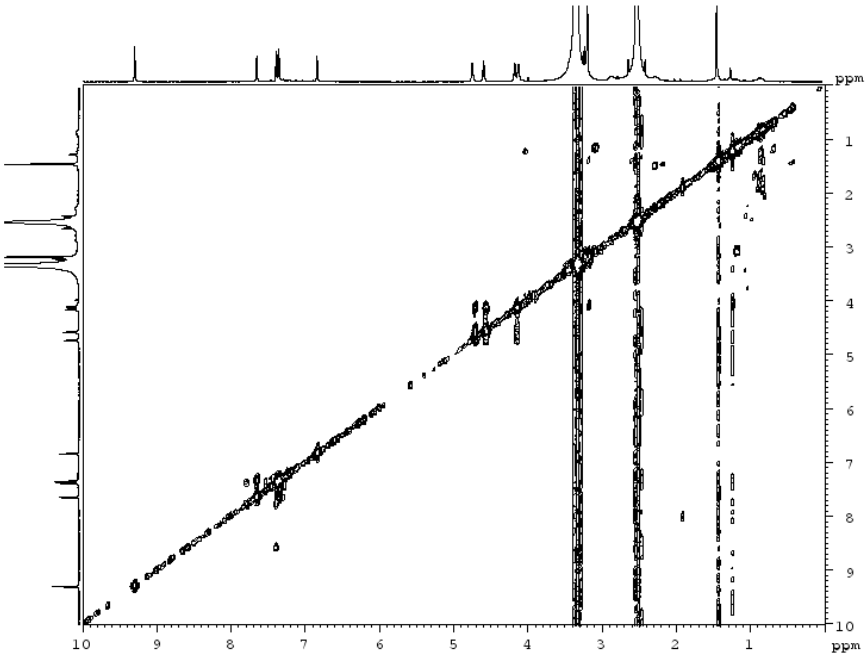

Supplementary figure 16. COSY spectrum (DMSO-d_6, 600 MHz) of arixanthomycin C (**3**).

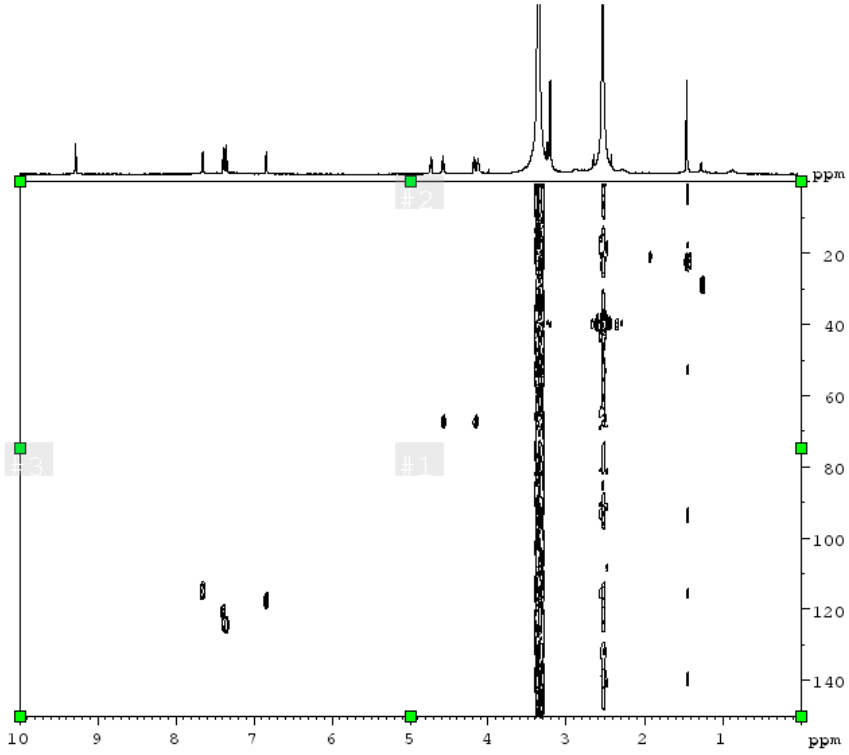

Supplementary figure 17. HMQC spectrum (DMSO-d_6, 600 MHz) of arixanthomycin C (**3**).

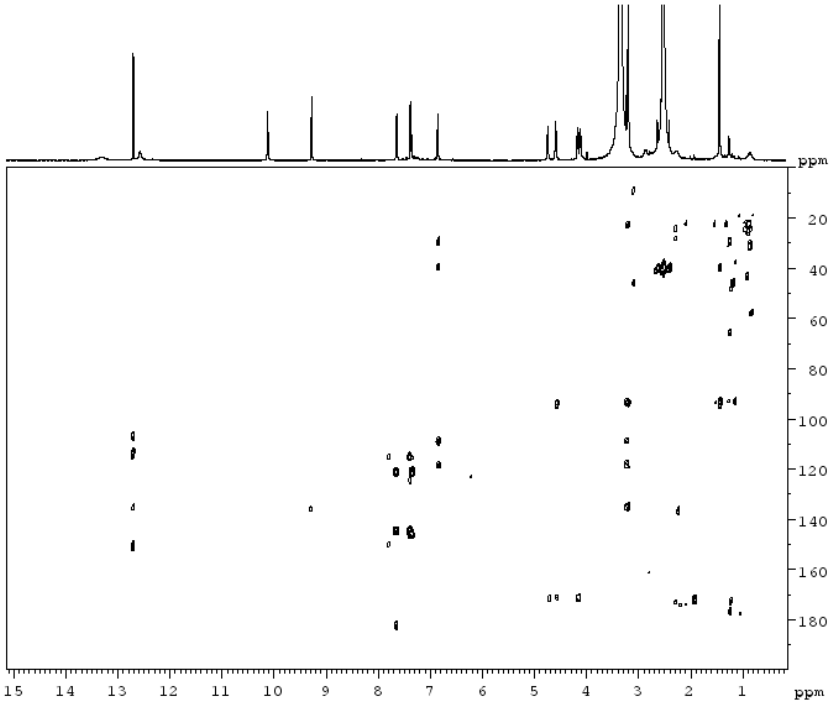

Supplementary figure 18. HMBC spectrum (DMSO-d_6, 600 MHz) of arixanthomycin C (**3**).